**Electronic Supplementary material**

# Bimetallic (Ni/Co) metal-organic framework with excellent oxidase-like activity for colorimetric sensing of ascorbic acid

Jing Wan, Jian-Mei Zou*, Shu-Jing Zhou, Feng-Lan Pan, Fei Hua, Yu-Lan Zhang, Jin-Fang Nie, Yun Zhang*

Guangxi Key Laboratory of Electrochemical and Magnetochemical Function Materials, College of Chemistry and Bioengineering, Guilin University of Technology, Guilin 541004, P. R. China

*Corresponding author. E-mail address: 2019136@glut.edu.cn (Jianmei Zou), zy@glut.edu.cn (Yun Zhang).
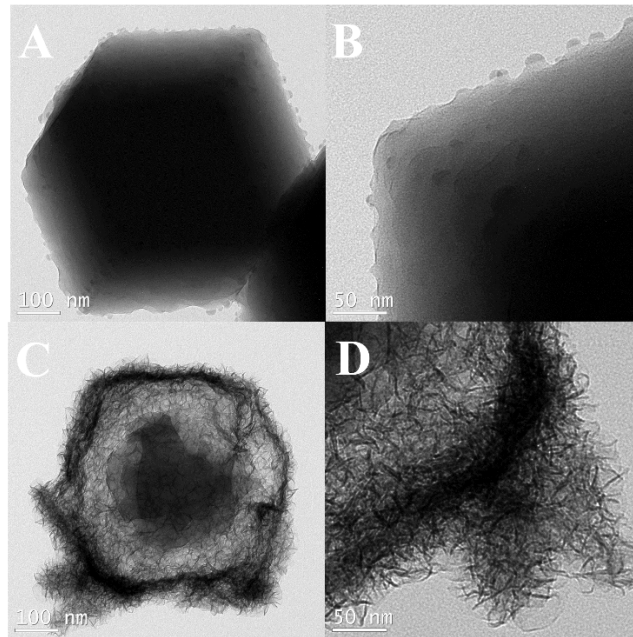
**Fig. S1** TEM images of ZIF-67 (A and B) and Ni/Co-MOF (C and D) under different magnifications.
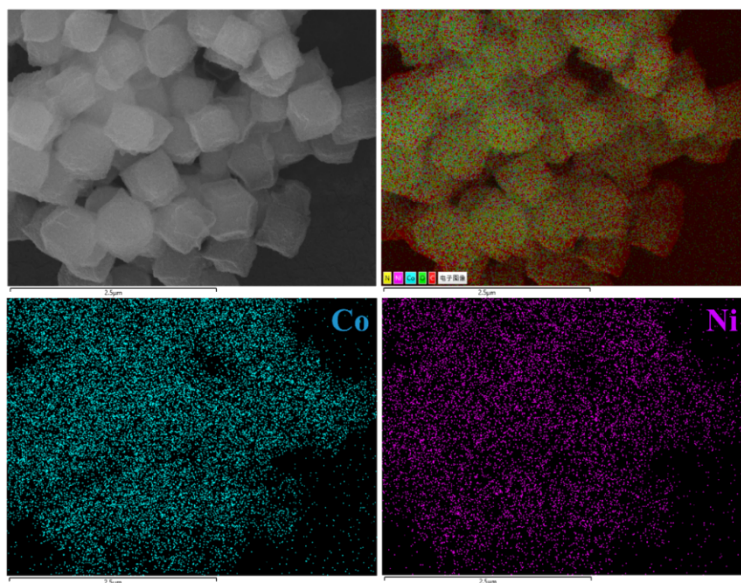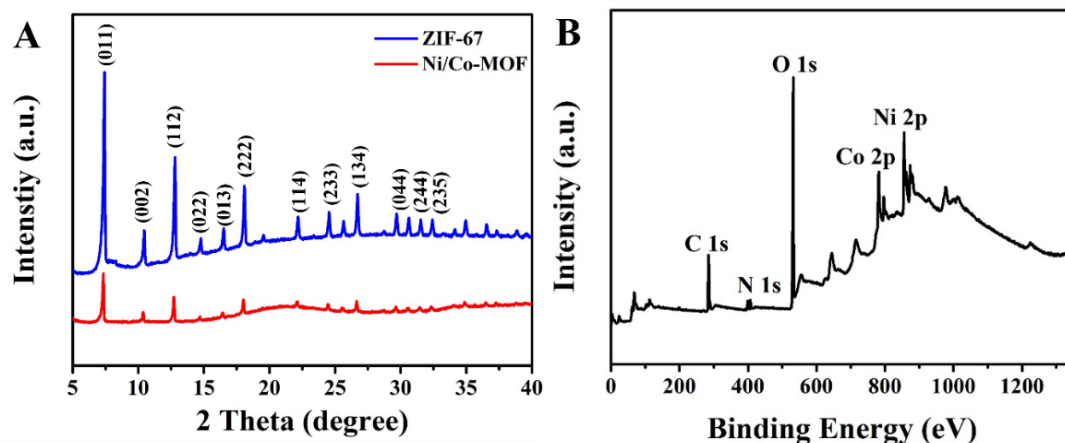


**Fig. S2** EDS mappings of Ni/Co-MOF.

**Fig. S3** (A) XRD patterns of ZIF-67 and Ni/Co-MOF. (B) XPS survey spectrum of Ni/Co-MOF.
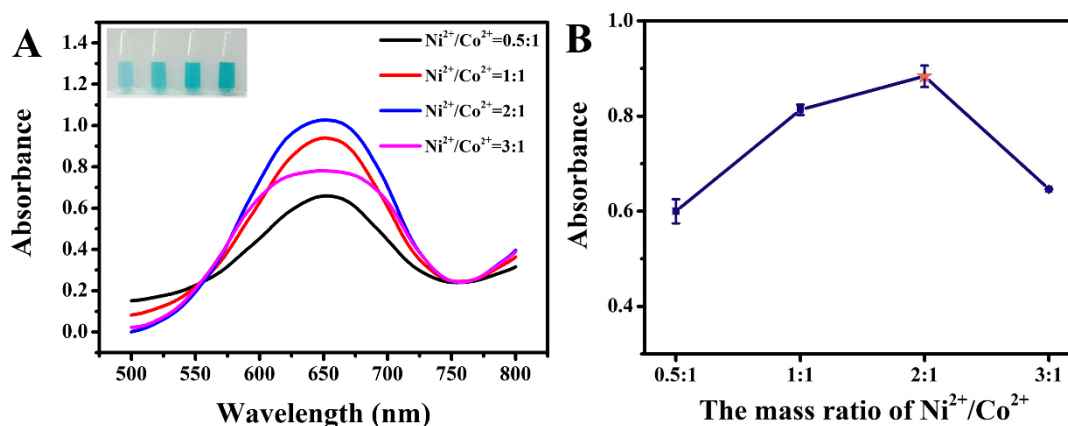


**Fig. S4** Effect of the $Ni^{2+}:Co^{2+}$ mass ratio on the catalytic activity of Ni/Co-MOF. Reaction conditions: 400 μM TMB, 400 μg $mL^{-1}$ Ni/Co-MOF, 0.2 mM NaAc-HAc buffer (pH 4.0), 15 min, 25 °C. (A) UV-vis absorption spectra and visual color changes of TMB in the reaction systems with various catalysts. (B) Corresponding line chart of (A). The error bars represent the standard deviations for three repeated experiments.
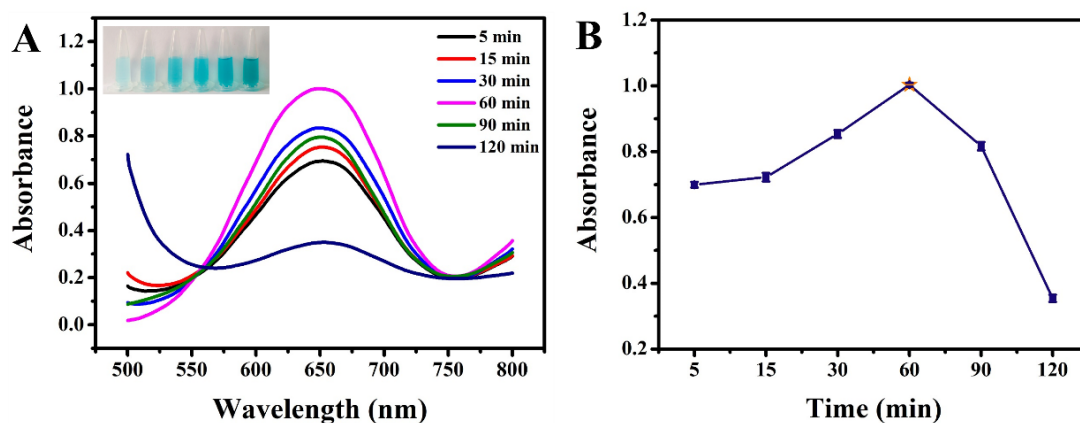
**Fig. S5** Effects of synthesis time on the catalytic activity of Ni/Co-MOF. (A) UV-vis absorption spectra and visual color changes of TMB in the reaction systems containing Ni/Co-MOF synthesized over 5, 15, 30, 60, 90, and 120 min. (B) Corresponding line chart of (A). The error bars represent the standard deviations for three repeated experiments.
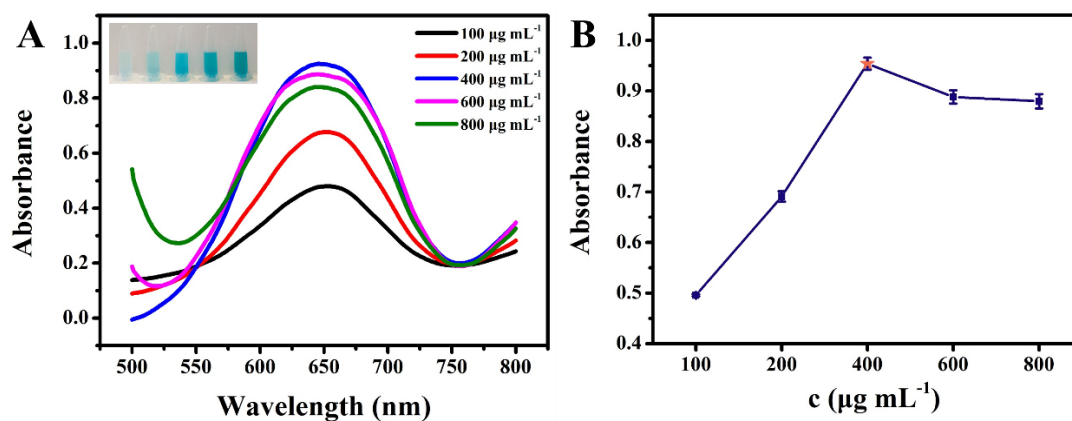


**Fig. S6** (A) UV-vis absorption spectra and visual color changes of TMB in reaction systems containing 100, 200, 400, 600, and 800 μg mL$^{-1}$ Ni/Co-MOF. (B) Corresponding line chart of (A). Reaction conditions: pH 4.0, reaction time 15 min, temperature 25 °C, and TMB concentration 400 μM, unless otherwise stated.
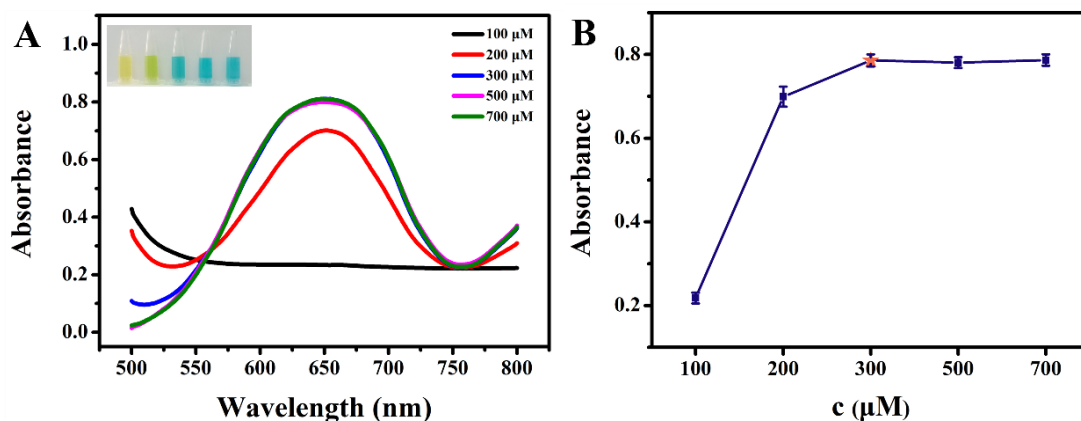
**Fig. S7** (A) UV-vis absorption spectra and visual color changes of TMB in reaction systems containing 100, 200, 300, 500, and 700 μM TMB. (B) Corresponding line chart of (A). Reaction conditions: Ni/Co-MOF concentration 400 μg mL$^{-1}$, pH 4.0, reaction time 15 min, and temperature 25 °C, unless otherwise stated.
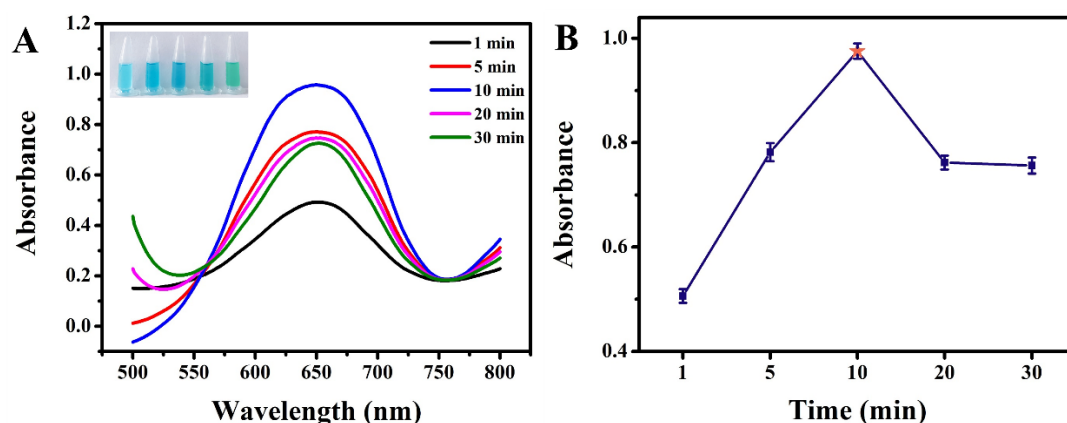


**Fig. S8** (A) UV-vis absorption spectra and visual color changes of TMB after 1, 5, 10, 20, and 30 min of reaction. (B) Corresponding line chart of (A). Reaction conditions: Ni/Co-MOF concentration 400 μg mL$^{-1}$, pH 4.0, temperature 25 °C, and TMB concentration 300 μM, unless otherwise stated.
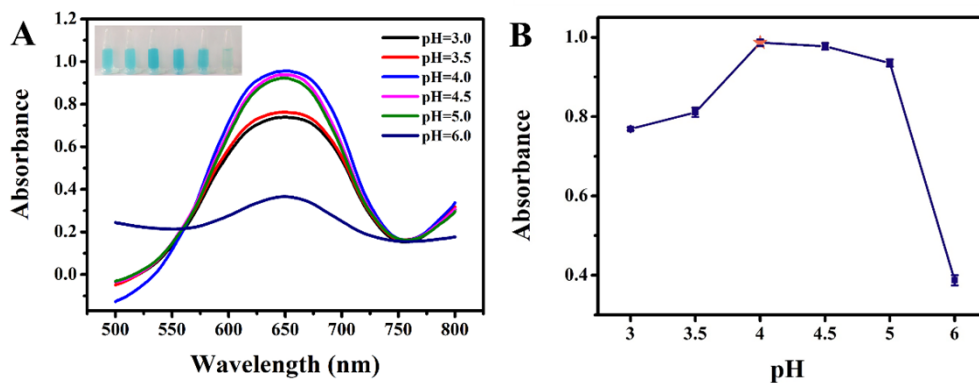
**Fig. S9** (A) UV-vis absorption spectra and visual color changes of TMB in reaction systems with pH 3, 3.5, 4, 4.5, 5, and 6. (B) Corresponding line chart of (A). Reaction conditions: Ni/Co-MOF concentration 400 μg mL$^{-1}$, reaction time 10 min, temperature 25 °C, and TMB concentration 300 μM, unless otherwise stated.



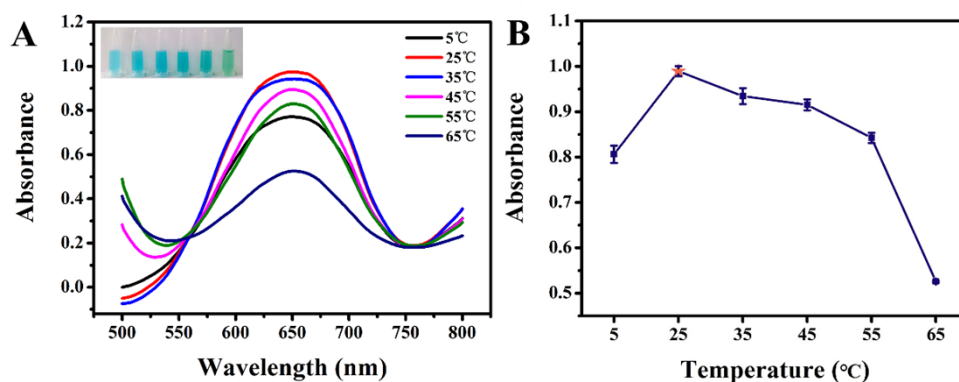**Fig. S10** (A) UV-vis absorption spectra and visual color changes of TMB in reaction systems at 5, 25, 35, 45, 55, and 65 °C. (B) Corresponding line chart of (A). Reaction conditions: Ni/Co-MOF concentration 400 μg mL$^{-1}$, pH 4.0, reaction time 10 min, and TMB concentration 300 μM, unless otherwise stated.

**Table S1.** The kinetic parameters of different catalysts

| Nanomaterials | $K_m$ (mM) | $V_{max}$ ($10^{-8}$ M s$^{-1}$) | References |
|---|---|---|---|
| Ni-MOF | 0.365 | 6.53 | 1 |
| GOx@Fe-BTC | 0.280 | 4.20 | 2 |
| MIL-100（Fe） | 0.424 | 2.10 | 3 |
| HRP | 0.434 | 10.0 | 4 |
| Ni/Co-MOF | 0.255 | 1.35 | This Work |

**Table S2.** Comparison of different colorimetric methods used for AA detection

| Catalyst | Linear rang (μM) | Detection limit (μM) | References |
|---|---|---|---|
| Fe/Co NPs | 0.5-28 | 0.380 | 5 |
| Fe-Mn bimetallic | 8-56 | 0.880 | 6 |
| Cu-Ag/rGO | 0.5-30 | 3.600 | 7 |
| Pt/CeO$_2$ | 0.5-30 | 0.080 | 8 |
| CuO/Pt | 1-600 | 0.796 | 9 |
| Ni/Co-MOF | 0.015-50 | 0.004 | This Work |

**Table S3.** Detection of AA contents in human serum and fruit juice samples

| Sample | Added (μM) | Total found (μM) | Recovery (%) | RSD(%) (n=3) |
|---|---|---|---|---|
| Human serum | 0 | 5.26 | / | 5.35 |
|  | 0.2 | 5.44 | 91.07 | 1.32 |
|  | 2 | 7.14 | 93.81 | 1.11 |
|  | 20 | 25.30 | 100.18 | 8.48 |
|  |  |  |  |  |
| Fruit juice | 0 | 6.29 | / | 3.13 |
|  | 0.2 | 6.48 | 95.31 | 0.31 |
|  | 2 | 8.37 | 103.99 | 1.71 |
|  | 20 | 26.60 | 101.53 | 1.90 |

**References**

(1) J. Chen, Y. Shu, H. Li, Q. Xu and X. Hu, *Talanta*, 2018, **189**, 254-261.

(2) Z. Zhao, J. Pang, W. Liu, T. Lin, F. Ye and S. Zhao, *Mikrochim. Acta.*, 2019, **186**, 295.

(3) A. H. Valekar, B. S. Batule, M. I. Kim, K. H. Cho, D. Y. Hong, U. H. Lee, J. S. Chang, H. G. Park and Y. K. Hwang, *Biosens. Bioelectron.*, 2018, **100**, 161-168.

(4) J. Yang, M. Cho and Y. Lee, *Biosens. Bioelectron.*, 2016, **75**, 15-22.

(5) T. Wu, Z. Ma, P. Li, M. Liu, X. Liu, H. Li, Y. Zhang and S. Yao, *Talanta*, 2019, **202**, 354-361.

(6) Y. Han, L. Luo, L. Zhang, Y. Kang, H. Sun, J. Dan, J. Sun, W. Zhang, T. Yue and J. Wang, *Lwt*, 2022, **154**.

(7) G. Darabdhara, B. Sharma, M. R. Das, R. Boukherroub and S. Szunerits, *Sens. Actuators B Chem.*, 2017, **238**, 842-851.

(8) X. Liu, X. Wang, C. Qi, Q. Han, W. Xiao, S. Cai, C. Wang and R. Yang, *Appl. Surf. Sci.*, 2019, **479**, 532-539.

(9) X. Wang, Q. Han, S. Cai, T. Wang, C. Qi, R. Yang and C. Wang, *Analyst*, 2017, **142**, 2500-2506.